

# Resonant effects on two-photon photoemission spectroscopy: Linewidths and intensities of occupied and unoccupied features for lead phthalocyanine films on graphite

M. Shibuta, K. Yamamoto, K. Miyakubo, T. Yamada, and T. Munakata\*

*Graduate School of Science, Osaka University, Toyonaka, Osaka 560-0043, Japan*

(Received 17 December 2009; revised manuscript received 15 February 2010; published 15 March 2010)

Two-photon photoemission (2PPE) spectroscopy has been performed for lead phthalocyanine films on graphite surface. Fully resolved occupied and unoccupied levels and resonant optical transitions between them are characteristics of the film surface [Phys. Rev. B **77**, 115404 (2008)]. 2PPE peaks due to photoemission from normally unoccupied levels ( $1\omega$  peaks) and those due to coherent two-photon process from occupied levels ( $2\omega$  peaks) show unexpected variations in intensities and widths when the pump photon energy crosses the resonances. At around a resonance between molecule-derived levels, we find an intensity switching in which only the  $2\omega$  peak appears at photon energy below the resonance, and at above the resonance, the  $1\omega$  peak becomes prominent and the  $2\omega$  peak becomes very weak. The  $1\omega$  peak is broadened with increasing photon energy. These results cannot be interpreted by a simple energy level scheme, and point to further understanding of 2PPE process. Temperature dependence reveals the origin of indirect transitions involving the unoccupied substrate  $\pi$  band. We also demonstrate that resonant 2PPE spectroscopy is effective to probe deeper occupied levels which are not well resolved in one-photon photoemission.

DOI: [10.1103/PhysRevB.81.115426](https://doi.org/10.1103/PhysRevB.81.115426)

PACS number(s): 73.20.-r, 79.60.Dp

## I. INTRODUCTION

The electronic structure and the excited electron dynamics in the vicinity of the Fermi level ( $E_F$ ) at interfaces between organic thin films and inorganic substrates are the key issues to understand the functionalities of organic films. Though occupied energy levels have been extensively studied by both experimental and theoretical works,<sup>1,2</sup> investigation for unoccupied levels are still challenging.<sup>3,4</sup> Two-photon photoemission (2PPE) spectroscopy based on ultrafast laser pulses is a promising method to probe the unoccupied levels and electron dynamics in the levels.<sup>3-6</sup> In 2PPE, a first light pulse excites electron from an occupied level to an unoccupied level. The normally unoccupied level is probed by photoemission with the second pulse (denoted as  $1\omega$  process). In one-color 2PPE experiment, the final energy of photoelectron  $E_K$  from  $1\omega$  process is written as

$$E_K = h\nu + E_m, \quad (1)$$

where  $h\nu$  is the photon energy and  $E_m(>0)$  is the energy of the unoccupied level with respect to  $E_F$ . The two-step process competes with the coherent two-photon process (denoted as  $2\omega$  process) which results in the photoelectron of

$$E_K = 2h\nu + E_i, \quad (2)$$

where  $E_i(<0)$  is the initial energy of the occupied level. One of the key advantages of 2PPE spectroscopy is the competition of the two processes. From the  $1\omega$  and  $2\omega$  peaks we can know the occupied and unoccupied levels at the same time. With photon energy of  $E_m - E_i$ , 2PPE signal is resonantly enhanced. Optical transition probability between the levels is important to understand the character of the electron wave functions. The photon energy dependence of the 2PPE signals due to  $1\omega$  and  $2\omega$  processes around the resonance has been studied by several theoretical works.<sup>7-11</sup> The theoretical results were carefully compared with experiments for the resonance between the occupied Shockley state and the first

image potential state (IPS) of Cu(111) surface.<sup>5,7,12</sup> On the other hand, experiments for different systems showed resonance behaviors deviated from the theories.<sup>13-15</sup> Understanding of the resonance behavior is essentially important to know the physical meaning of the unoccupied level detected by 2PPE experiment. The issue is especially serious for organic films in which addition or removal of electron in/from a molecular orbital causes significant change of the energy levels.

Here, we extend our former works on 2PPE of lead phthalocyanine (PbPc) films formed on a substrate of highly oriented pyrolytic graphite (HOPG).<sup>16,17</sup> We have resolved occupied levels due to the highest occupied molecular orbital (HOMO) and the next HOMO (HOMO-1). Also clearly resolved were the molecule-derived unoccupied levels (denoted as LUMO, LUMO+1, LUMO+2 in the order of energy) and the first IPS's on HOPG and on the PbPc films. In addition, a resonance between HOMO and LUMO+2, as well as that between HOMO and the IPS were observed at  $h\nu=4.3$  eV and 4.8 eV, respectively.<sup>16</sup> The system which involves two resonant excitations is a highly suitable example for detailed analysis of the resonance in 2PPE. We have measured 2PPE spectra for 1 monolayer (ML) films of PbPc on HOPG with improved signal-to-noise ratio. From the photon energy and temperature dependence of the peak profiles and the intensities, we analyze excitation processes in 2PPE spectroscopy, and present unresolved problems for 2PPE process.

## II. EXPERIMENT

In our former 2PPE work for PbPc films, we employed a microspot method in which laser radiation was focused on the sample to the spot of 0.6  $\mu\text{m}$  diameter.<sup>16</sup> The microspot method was effective to selectively observe laterally homogeneous surface areas, while the number of photoelectrons from the small probe areas was limited to suppress the space

charge effect.<sup>18</sup> In this work, the laser light was focused with a concave mirror of 35 cm focal length onto the sample surface in an ultrahigh vacuum (UHV) chamber at the incident angle of 60°. With the large light spot size of about 80  $\mu\text{m}$  diameter, the space charge effect was easily avoided with higher photoelectron intensity. In cost of the spatial resolution, signal to noise ratio of 2PPE spectrum was fairly improved compared to the microspot configuration.<sup>17</sup> We disregarded the lateral inhomogeneity of the films in this work because we have found in our former works that highly uniform 1 ML films were made by a suitable annealing process.<sup>16,19</sup> Note that formation of the uniform films was achieved only for 1 ML coverage, and was not for sub-ML films. Annealed sub-ML films seemed to be homogeneous when the surface image was measured with photoemission from the HOMO band,<sup>19</sup> but they were not homogeneous when the unoccupied levels were measured with the microspot-2PPE. The inhomogeneity of unoccupied levels will be discussed elsewhere. The light source of the 2PPE experiments was the *p*-polarized third harmonics (4.04–4.77 eV) of a tunable titanium sapphire laser. Repetition rate and pulse width of the third harmonics were 80 MHz and 100 fs, respectively. The power of the incident light was controlled to be less than 0.19 nJ/pulse. Photoelectrons emitted to the surface normal were detected with a hemispherical energy analyzer (VG-CLAM4 with nine channeltrons detector) of 20 meV resolution. The analyzer was modified to limit the electron acceptance angle to be  $\pm 1^\circ$ .

HOPG was cleaved in air and heated in UHV at 670 K for more than 50 h. Cleanliness of the surface was confirmed by the work function (4.45 eV) and the width of the  $n=1$  IPS peak. The IPS peak was narrower than 140 meV.<sup>16</sup> Purified PbPc was deposited by sublimation on the HOPG surface in an UHV preparation chamber with a rate of 0.05 nm/min as monitored by a quartz microbalance. The deposition and annealing conditions were similar to those in the former works.<sup>16,19</sup> The coverage was determined from the work function change. The well ordered 1 ML films were formed by annealing the deposited films of 0.4 nm thickness at 370 K for 1 h. The work function was 4.27 eV for the 1 ML film. The decrease in the work function is due to the uniform dipole layer at the interface.<sup>20</sup>

### III. RESULTS

#### A. General spectral features for 1 ML films

The 2PPE spectrum for the 1 ML film measured at  $h\nu = 4.65$  eV is compared with a one-photon photoemission (1PPE) spectrum in Fig. 1. The sample was at room temperature (RT). The 1PPE spectrum,<sup>16</sup> measured by the microspot configuration with  $h\nu = 8.86$  eV, reproduces 1PPE spectra with He-I resonance line<sup>17,20</sup> except for slight broadening due to the space charge effect. Molecules in the annealed 1 ML films are lying flat on the substrate directing Pb atoms to vacuum side.<sup>20</sup> In the 2PPE spectrum, the peaks due to the first ( $n=1$ ) IPS on the film, the HOMO derived occupied level, and the LUMO+2 derived unoccupied level are clearly observed. The HOMO derived peak is at  $-1.33$  eV for both 2PPE and 1PPE spectra. The vibronic structure appears as a

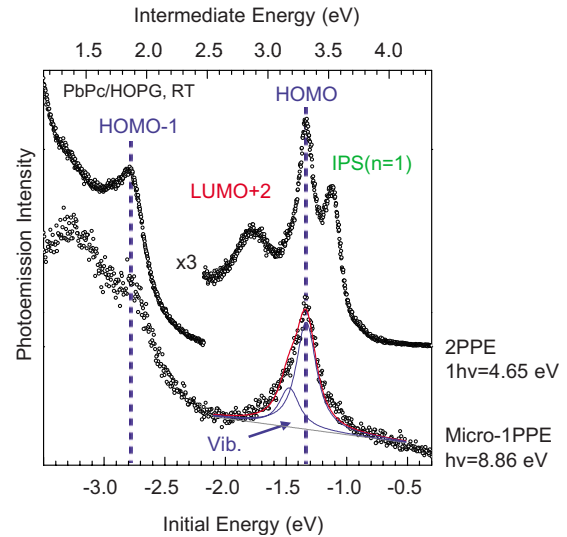


FIG. 1. (Color online) 2PPE (top) and micro-1PPE (bottom) spectra for the well annealed 1 ML PbPc film on HOPG. The photon energies are shown at right-hand side. The upper horizontal axis is the intermediate energy (final energy- $1h\nu$ ) for 2PPE. The 2PPE trace in the right hand is magnified by a factor of 3 to that in the left-hand side. Peaks due to IPS and molecule-derived levels (HOMO, LUMO+2 and HOMO-1) are clearly resolved. The HOMO and HOMO-1 peaks are at  $-1.33$  and  $-2.78$  eV initial energy for both spectra. Note the largely different appearance of the HOMO-1 feature: the sharp peak in the 2PPE is a contrast to the broad shoulder in the 1PPE result.

shoulder at  $-1.47$  eV in the 1PPE spectrum, while it is very weak in the 2PPE result. The weak vibronic structure is due to the nuclear motion in the electronic excited state associated with the LUMO+2 level.<sup>17</sup> The HOMO-1 derived peak appears at  $-2.78$  eV for both spectra, but the spectral shapes are largely different. The peak is sharp in 2PPE when compared with the broad shoulder in 1PPE. The broad 1PPE feature reproduces that of Ref. 20 measured with  $h\nu = 21.2$  eV.

The 2PPE spectra measured at different photon energies for the film of 90 K are shown in Fig. 2. At photon energy higher than the work function of 4.27 eV, strong 1PPE is observed at the left-hand edge of Fig. 2. Though the 1PPE signal increases the low energy background, it causes no significant influence on the 2PPE features. The relatively low disturbance by the 1PPE is partly due to the uniformity of the present sample surface. The 2PPE peaks were assigned previously as indicated.<sup>16</sup> According to a DFT calculation (Gaussian 03, B3LYP with LANL2DZ basis set) for a free molecule, HOMO-1 is mainly composed of orbitals of Pb atom ( $A_1$  symmetry in  $C_{4v}$  point group), and other occupied and unoccupied orbitals, HOMO ( $A_2$ ), LUMO (E), LUMO+1(E), and LUMO+2 ( $B_1$ ), are composed of  $\pi$ -orbitals of phthalocyanine ring. The LUMO and LUMO+1 levels degenerate in a free molecule. The degeneracy is lifted by the adsorption.<sup>16</sup> The split levels appear as two peaks at 0.71 and 0.88 eV, labeled as L0 and L1, respectively. The splitting indicates a symmetry reduction in PbPc molecule by adsorption. The symmetry reduction of phthalocyanine ring from fourfold symmetry was reported for SnPc on Ag(111) and

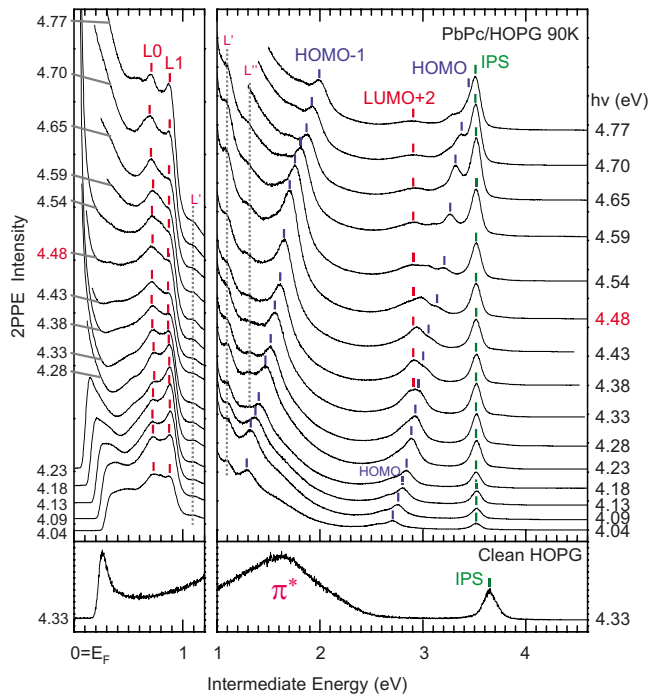


FIG. 2. (Color online) Photon energy dependence of 2PPE spectra for 1 ML PbPc/HOPG measured at 90 K. The photon energies are shown at both left and right-hand sides of the spectra. The bottom spectrum is for the clean HOPG measured at RT. The horizontal axis is the intermediate energy. The HOMO-1 peak is enhanced at 1.7 eV intermediate energy. In addition to the peaks appeared in Fig. 1, the LUMO and LUMO+1 derived levels appear as split components, labeled L0 and L1. The intensity ratio between L0 and L1 changes as the change of the photon energy. Weak features labeled as  $L'$  and  $L''$  are left unassigned.

CuPc on Cu(111) by scanning tunneling microscopy works.<sup>21,22</sup>

### B. HOMO-1 peak

The HOMO-1 peak in Fig. 2 is enhanced at  $h\nu = 4.48$  eV. From the initial energy of the HOMO-1 peak of  $-2.78$  eV, the intermediate energy for the enhancement is  $1.70 (=4.48 - 2.78)$  eV. In order to confirm the enhancement of the HOMO-1 peak, expanded spectra measured at RT are shown in Fig. 3. The HOMO-1 peak is enhanced at photon energy of 4.48 eV, reproducing Fig. 2. The peak width is not strongly dependent on the photon energy. By comparing Figs. 2 and 3, we identified no significant temperature dependence for the HOMO-1 enhancement. The enhancement is discussed in Sec. IV A.

### C. LUMO+2, HOMO and IPS peaks

The LUMO+2, HOMO, and IPS peaks appear at the energy region above 2.5 eV as can be seen in Fig. 2. The photon energy dependence of their intensities and widths are rather complicated. The HOMO derived peak becomes stronger as the photon energy increased from 4.04 to 4.23 eV. At  $h\nu = 4.23$  eV, the peak is sharp and intense: the enhancement

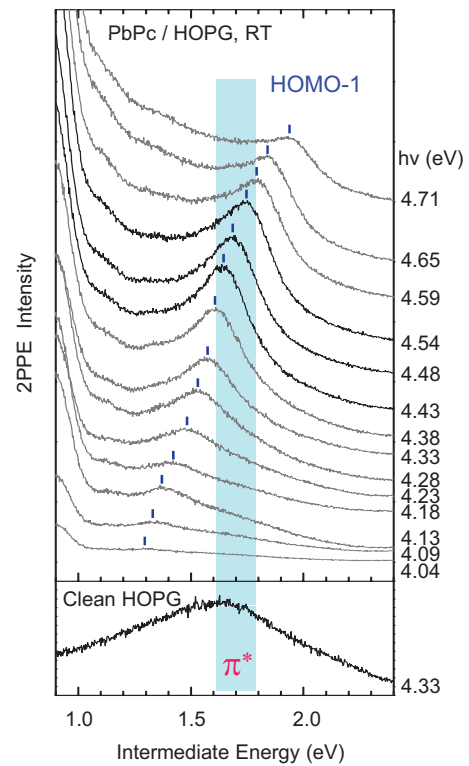


FIG. 3. (Color online) Close up of the HOMO-1 derived peak measured at RT. The photon energies are indicated at right-hand side. The bottom trace is the 2PPE spectrum for the clean HOPG substrate. The broad peak for HOPG at 1.7 eV intermediate energy, marked by a vertical bar, is due to the unoccupied  $\pi^*$  band of graphite. The enhancement of the HOMO-1 peak at 1.7 eV intermediate energy is due to the resonance with the  $\pi^*$  band. Note that the  $\pi^*$  peak is not visible for the PbPc film.

is due to the resonance between the HOMO and LUMO+2 derived levels.<sup>16</sup> Optical transition between HOMO ( $A_2$ ) and LUMO+2 ( $B_1$ ) is forbidden for a free molecule. The observed resonance indicates again the symmetry reduction of adsorbed PbPc. At  $h\nu > 4.33$  eV, the LUMO+2 component is separated from the HOMO component. The overlapped peak is mainly composed of the LUMO+2 component, and the HOMO component is resolved as a weak shoulder at  $h\nu = 4.38$  and 4.43 eV. The intensity of the HOMO peak is switched to that of the LUMO+2 peak when the photon energy increases across the resonance energy. We denote the sudden intensity changes as “intensity switching.” The intensity switching is clearly seen in Fig. 4 where selected spectra are shown in an expanded scale. The HOMO peak becomes strong again at  $h\nu > 4.48$  eV. The intensity increase is due to the resonance between the HOMO derived level and IPS.<sup>16</sup> The LUMO+2 peak is not observed at photon energies lower than 4.18 eV. The peak becomes prominent at the HOMO-LUMO+2 resonance and becomes gradually weaker as the photon energy increases. The width of the LUMO+2 peak becomes wider with increasing photon energy (see Fig. 4). In contrast to these molecule-derived peaks, the IPS peak appears for all the spectra and becomes stronger with increasing photon energy. The IPS peak nearly merges with the HOMO peak at  $h\nu = 4.77$  eV (the HOMO-IPS resonance).

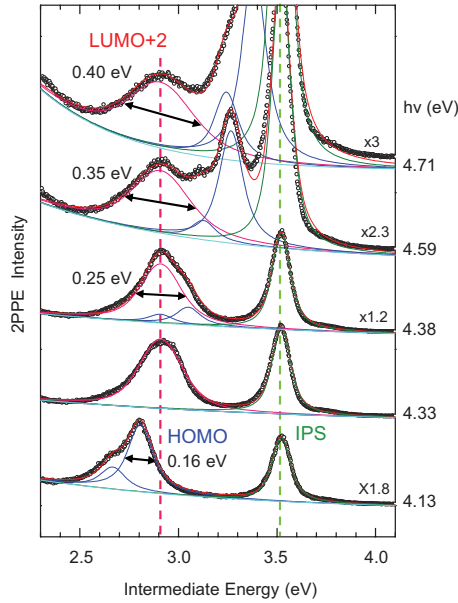


FIG. 4. (Color online) 2PPE spectra are fitted with Voigt functions for the IPS [green (gray)], HOMO [blue (black)], and LUMO+2 [pink (dark gray)] peaks. The photon energies are shown at the right-hand side. The magnification factors relative to the spectrum at  $h\nu=4.33$  eV are indicated at right-hand side. At  $h\nu=4.13$  eV, the width of the HOMO peak is 0.16 eV, and the LUMO+2 peak is not observed. The HOMO peak is much weaker than the LUMO+2 peak at  $h\nu=4.38$  eV. The LUMO+2 peak becomes broader as the photon energy increases. The widths are shown at left-hand sides of the LUMO+2 peaks.

The width of the IPS peak is almost constant throughout the photon energy region.

For a quantitative analysis, the 2PPE spectra are fitted with four Voigt functions and some characteristic results are shown in Fig. 4. The fitting was made as follows: the initial energies for the HOMO peak and its vibronic structure were fixed to  $-1.33$  and  $-1.47$  eV, respectively. The intermediate energies for the LUMO+2 and IPS peaks were also fixed to  $+2.91$  and  $+3.52$  eV, respectively. Thus the energy for the HOMO-LUMO+2 resonance is 4.24 eV, and that for the HOMO-IPS resonance, 4.85 eV. In order to reduce the number of adjustable parameters, the Lorentzian and Gaussian widths,  $W_L$  and  $W_G$ , of the IPS peak were fixed to 80 and 60 meV, respectively. The width parameters of the LUMO+2 peak were adjustable with equal  $W_L$  and  $W_G$ . The main HOMO peak was fitted with fixed  $W_G$  of 60 meV and adjustable  $W_L$ . The width parameters for the vibronic structure were set to be the same as those of the main HOMO peak. The fixed width parameters for the IPS and HOMO peaks were determined from the spectrum at  $h\nu=4.13$  eV.

The areas and full widths at half maxima (FWHMs) of the peaks are plotted against the photon energy in Fig. 5. At  $h\nu=4.28$  and 4.33 eV, the HOMO and LUMO+2 peaks are heavily overlapped, and the intensity and the width of the HOMO peak are not determined. The intensities at  $h\nu > 4.7$  eV are not very reliable because the photon energy is close to the limit of the tuning range of our laser. The variation in the intensities and the widths are discussed in Sec. IV B.

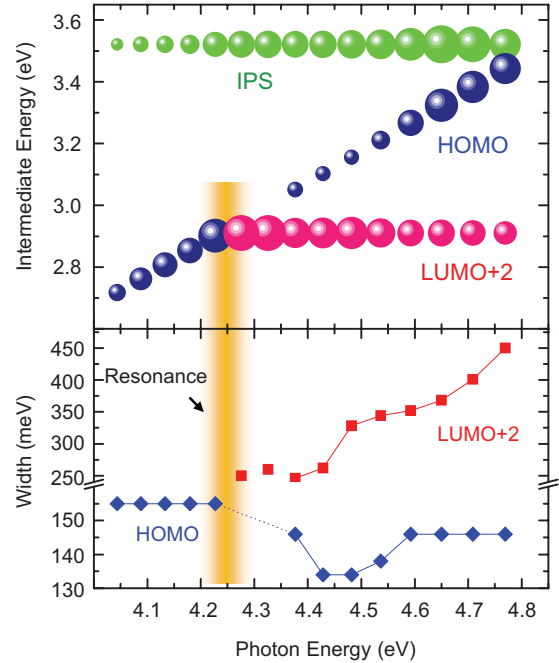


FIG. 5. (Color online) Fitted results for the spectra in Fig. 2. (top) The intensities of the HOMO, LUMO+2, and IPS peaks are represented against the photon energy by the areas of the blue (black), pink (dark gray), and green (gray) circles, respectively. (Bottom) The widths of the HOMO and LUMO+2 peaks are shown by (blue) diamonds and (red) squares, respectively. For  $h\nu=4.28$  and 4.33 eV, the width and intensity of the HOMO peaks are not determined. The width and intensity of the HOMO peak becomes narrower within a photon energy range up to 0.4 eV above the resonance. The LUMO+2 peak becomes broader as the photon energy increases. The HOMO-LUMO+2 resonance is marked by a vertical bar.

#### D. L0 and L1 features

The intensity ratio between L0 and L1 changes by increasing the photon energy (see Fig. 2). At  $h\nu=4.04$  eV, both peaks are weak and the L0 component is slightly stronger than the L1 component. The peaks become intense as the photon energy increases. The intensity of L0 is weaker than L1 at  $h\nu=4.18$ – $4.28$  eV. The L0 component becomes stronger again at  $h\nu > 4.33$  eV. At  $h\nu > 4.65$  eV, the further enhanced peaks shows slightly changed spectral shapes. The  $h\nu$  dependent of the L0 and L1 intensities is discussed in Sec. IV C. The weak peaks at 1.10 and 1.32 eV in Fig. 2, labeled as  $L'$  and  $L''$ , respectively, were not resolved in Ref. 16. The unoccupied levels for the  $L'$  and  $L''$  peaks should be another split components of the LUMO and LUMO+1, but are left unassigned here.

## IV. DISCUSSIONS

### A. HOMO-1 derived peak

The sharp HOMO-1 peak in the 2PPE spectra is a clear contrast to the shoulderlike feature in the 1PPE result. The enhancement of the HOMO-1 peak at the intermediate energy of 1.7 eV should be a resonance with an unoccupied level at the energy. In order to clarify the origin of the unoc-

cupied level, the 2PPE spectrum for the clean HOPG substrate measured at  $h\nu=4.33$  eV is shown at the bottoms of Figs. 2 and 3. The broad structure labeled as  $\pi^*$  is observed. The peak is located at around 1.7 eV as indicated by a bar in Fig. 3. Similar broad structure in a 2PPE spectrum of HOPG was reported and attributed to non- $k_{\parallel}$ -conserving transitions from the initial state into a high density of the unoccupied  $\pi^*$  band of graphite.<sup>23</sup>  $k_{\parallel}$  is the electron momentum parallel to the surface. Inverse photoemission works reported a nondispersing unoccupied level at similar energy.<sup>24–27</sup> Because the peak energy of the  $\pi^*$  structure is close to the intermediate energy for the HOMO-1 enhancement, we attribute the HOMO-1 enhancement to the resonance between the HOMO-1 level and the unoccupied  $\pi^*$  band of graphite.

The band structures and electron-phonon coupling in graphite have been extensively studied.<sup>23,28–31</sup>  $\pi$  band of graphite crosses  $E_F$  at  $K$  point forming so-called “Dirac cone.” The unoccupied part of the  $\pi$ -band ( $\pi^*$ ) below 2 eV is located in the momentum region from  $M$ ,  $K$ , to  $H$  points. The occupied and unoccupied  $\sigma$  bands are located below  $-4$  and above 4 eV, respectively. The energy region between  $-4$  and 4 eV at the  $\Gamma$  point of bulk graphite is in the band gap. We measured photoelectrons emitted normal to the surface, that is, we probed the  $\Gamma$ -point of the surface Brillouin zone. Photoelectrons detected at the surface normal direction should be generated by some indirect transitions. The origin of the indirect transition can be compared with the real intermediate states within the projected band gap known in the 2PPE works for Cu(111).<sup>32–34</sup> Petek discussed the role of phonon-assisted process as the origin of the real unoccupied states within the band gap.<sup>32</sup> In order to compare our HOPG result with the Cu(111) case, temperature dependence of 2PPE spectra is shown in Fig. 6(a). The intensity of the  $\pi^*$  structure for clean HOPG decreases at 90 K, suggesting that the  $\pi^*$  structure for clean HOPG is related with thermal phonon. Similarly to Cu(111), the broad  $\pi^*$ -structure at 1.7 eV for clean HOPG should arise from the phonon coupled states which are essentially the momentum integrated density of state of the unoccupied  $\pi^*$  band.

Another interesting feature of the  $\pi^*$  structure is that the peak of the substrate almost disappears for the 1 ML covered surface. The electron mean free path of the low energy photoelectrons is fairly longer than the thickness of the films. The disappearance of the  $\pi^*$  structure cannot be attributed to the attenuation of the photoelectrons by the films. In contrast to the clean HOPG in Fig. 6(a), the intensity of the HOMO-1 peak is insensitive to the temperature as shown in Fig. 6(b), suggesting that the thermal phonon is not contributing to the intensity of the HOMO-1 peak. The surface phonon of graphite should be largely disturbed by adsorbed PbPc, and the phonon-assisted process inducing the  $\pi^*$  structure for the clean surface becomes less effective. Then the  $\pi^*$  structure disappears for the PbPc covered surface. In place of the phonon-assisted process, we consider a role of electron scattering by PbPc molecules. In our preliminary work, the HOMO-1 band shows no significant dispersion. Photoexcitation from the HOMO-1 level to the  $\pi^*$  band occurs in proportional to the density of state of the  $\pi^*$  band. Photoelectron from the  $\pi^*$  band can be scattered by the molecules to the surface normal direction. The electron scattering should be

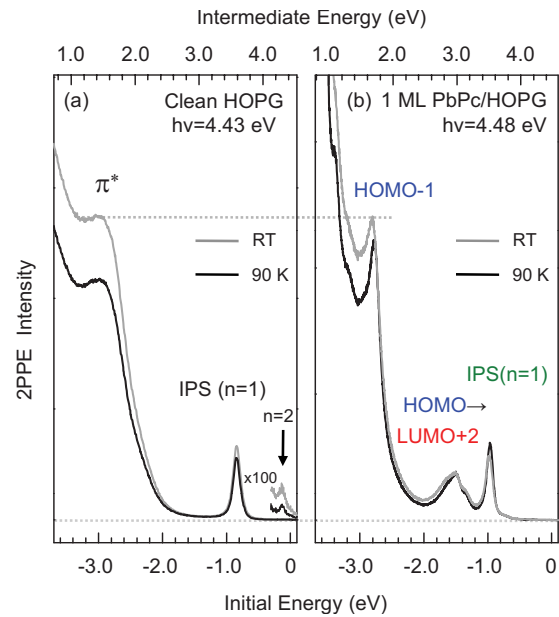


FIG. 6. (Color online) Temperature dependence of 2PPE spectra for (a) clean HOPG and (b) 1 ML PbPc/HOPG. The gray and black traces are for RT and 90 K, respectively. The RT spectra for (a) and (b) are normalized (gray horizontal line) to the intensities at the  $-2.8$  eV initial energy. For clean HOPG, the intensity of the  $\pi^*$  peak at around 1.7 eV intermediate energy decreases as temperature decreases, suggesting that the  $\pi^*$  peak arises from phonon-assisted process. The IPS peak also becomes weak by decreasing the temperature. On the other hand, the intensities of the HOMO-1 peak and the IPS peak for the film are nearly independent of the temperature. The low energy backgrounds in these spectra are higher than those in Figs. 2 and 3 because of the different experimental conditions.

effective in 2PPE when the electronic transition is coupled with the molecule, and the  $\pi^*$  band contributes to 2PPE only as the intermediate state for the HOMO-1 peak. The HOMO-1 peak is observed throughout the photon energy region of Figs. 2 and 3. The variation in the peak height with the photon energy reflects the density of state of the  $\pi^*$  band. The peak width shows no significant dependence on the photon energy. The resonance narrowing discussed in Sec. IV B does not occur because the width of the  $\pi^*$  band is fairly wider than that of the HOMO-1 level. Peak narrowing by energy filtering effect<sup>35</sup> known in resonant three-photon photoemission from Cu(001) is not the case of the present system in which the band width of the laser light ( $<20$  meV) is narrower than the widths of the relevant energy levels and the dispersion of the intermediate state is not important. Thus the peak width in Fig. 3 corresponds to the width of the HOMO-1 level. While we do not discuss the origin of the shoulderlike feature in 1PPE, 2PPE can resolve the HOMO-1 level clearer than 1PPE.

As can be seen in Fig. 6(a), the intensity of the IPS peak for HOPG decreases at low temperature, suggesting that the IPS peak is affected by thermal phonon. Because of the band gap at  $\Gamma$  point, the IPS for bare HOPG is excited by an indirect transition from occupied states at high momentum regions. The indirect transition becomes effective by

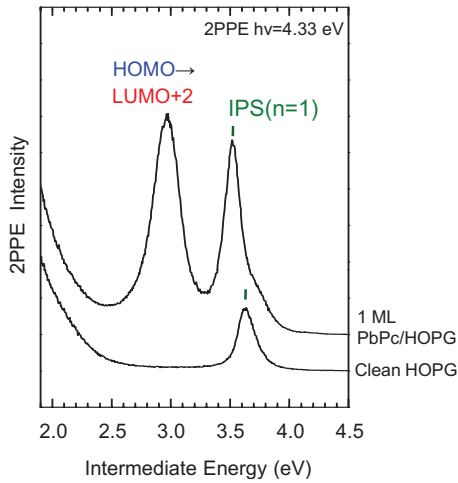


FIG. 7. (Color online) Close up of 2PPE spectra for clean HOPG (bottom) and the 1 ML PbPc/HOPG (top) measured at 4.33 eV photon energy, which is far from the HOMO-IPS resonance. The IPS peak for the film is significantly higher than that for the clean HOPG. The enhancement indicates that the IPS is hybridized with an unoccupied level of the PbPc film.

phonon-assisted momentum conservation. On the other hand, the IPS peak for the PbPc film is rather insensitive to the temperature. The IPS on the film is related with a molecule-derived unoccupied level as is discussed in Sec. IV B.

### B. HOMO, LUMO+2 and IPS peaks

The intensity of the IPS peak monotonically increases as the photon energy increases close to the HOMO-IPS resonance. The intensity increase indicates that electrons in the IPS are excited from both the HOMO level and the bulk band of graphite. It is interesting that the intensity of the IPS peak for the 1 ML PbPc film is higher than that for the clean HOPG as shown in Fig. 7. The binding energies from the vacuum level are 0.85 eV for the clean HOPG and 0.73 eV for the PbPc films, respectively. The increase in the intensity is not in accordance with the frequently used dielectric continuum model.<sup>36–39</sup> When the film acts as the dielectric isolation layer, the wave function of the IPS penetrates into the substrate by less extent and the intensity of the IPS peak becomes weaker than that for the clean surface. On the other hand, the increase in the intensity of the IPS peak indicates that the PbPc film is not the simple isolation layer. As an origin of the enhancement, we consider a hybridization of the IPS with a molecule-derived unoccupied level. Our DFT calculation<sup>16</sup> for a free molecule shows that LUMO+3 or 4 is located close to the IPS. By mixing of the molecule-derived unoccupied level with IPS, the IPS wave function is not dumped in the film. Then the penetration of the IPS wave function into the substrate is enhanced, and the IPS peak becomes stronger. The mixing also causes the HOMO-IPS resonance by the intramolecular transition.

It is interesting that the LUMO+2 peak is observed only at photon energies higher than the HOMO-LUMO+2 resonance at  $h\nu=4.24$  eV. The width of the HOMO peak is 0.16 eV at photon energy below the resonance and the width of

the LUMO+2 peak is about 0.25 eV at  $h\nu=4.38$  eV (see Figs. 4 and 5). Simply considering that the intensity variation in the unoccupied peak around the resonance is determined by a convolution of the occupied and unoccupied density of states, the LUMO+2 peak is expected to appear at the photon energy region higher than  $4.04 [=4.24 - (0.16 + 0.25)/2]$  eV. But no trace of the LUMO+2 peak is observed at the photon energy region from 4.04 to 4.18 eV. On the other hand, the intensity of the HOMO peak increases as  $h\nu$  increases from 4.04 to 4.18 eV, reflecting the resonance. As can be seen in Figs. 4 and 5, the HOMO peak suddenly becomes very weak as the photon energy exceeds the resonance, and the LUMO+2 contribution suddenly becomes prominent at  $h\nu=4.23$  eV. The intensity switching between the HOMO and LUMO+2 peaks is strange in the view of the simple resonance.

According to 2PPE results for Cu(111), the  $n=1$  IPS peak due to  $1\omega$  process is observed even at photon energy lower than the resonance between the occupied Shockley state and IPS.<sup>7,12,13</sup> The intensity variations in the IPS peak due to  $1\omega$  process and the Shockley state peak due to  $2\omega$  process are symmetric with respect to the resonant photon energy. The intensity variation as a function of the pump photon energy has been discussed based on the dephasing process.<sup>7–10,12</sup> When the present PbPc results are compared with the known trend, the intensity variation around the HOMO-IPS resonance may be viewed as to be similar to the Cu(111) case: both the HOMO peak ( $2\omega$ ) and the IPS peak ( $1\omega$ ) become stronger as the photon energy increasing closer to the HOMO-IPS resonance. In contrast to the HOMO-IPS resonance, the intensity variations around the HOMO-LUMO+2 resonance are asymmetric: the intensity of the HOMO ( $2\omega$ ) peak is switched to the LUMO+2 ( $1\omega$ ) peak at the resonance. Similar intensity switching at the resonance was reported for several transitions of Si surfaces.<sup>13–15</sup> The asymmetric intensity variation is not specific to the present molecular film. The detailed mechanism for the intensity variation in 2PPE peaks awaits for further understanding on the 2PPE process as was suggested by Weinelt.<sup>13,40</sup>

The LUMO+2 peak due to  $1\omega$  process is observed at photon energies far above the resonance. If only the HOMO level was the initial state, energy conservation is not fulfilled. A possible mechanism may be an optical transition from the HOMO level to some resonantly excited state followed by relaxation to populate the LUMO+2 level. But such an excited state is not observed and is not very probable for the film with the clearly resolved energy levels. Rather, we consider a contribution of occupied bulk bands of the substrate as the initial state. The contribution is mentioned below when the width of the LUMO+2 peak is discussed.

Figure 5 shows that the width of HOMO is 0.16 eV at  $h\nu < 4.23$  eV and becomes narrower to 0.13 eV at the resonance. It becomes about 0.15 eV again at  $h\nu > 4.59$  eV. According to Ueba's theory of resonance narrowing,<sup>8</sup> the widths of 2PPE peaks become narrower by interference of  $1\omega$  and  $2\omega$  processes, and the peak profiles at the resonance are determined by the product of the occupied and unoccupied density of states. Taking the widths of the HOMO and LUMO+2 levels to be 0.16 and 0.25 eV, respectively, the width of the product function is estimated to be about 0.13 eV. The

value close to the observed width supports the narrowing mechanism. We present the estimated value with reservation, because the functional forms of the intrinsic density of states are not accurately known. The narrowing is observed at the photon energy range of about 0.4 eV wide. The energy range should be correlated with the widths of the HOMO and LUMO+2 levels and is similar to the photon energy window of 0.4 eV for the suppression of the HOMO vibronic structure.<sup>17</sup> Though the resonance narrowing should occur symmetrically around the resonance, Fig. 5 shows that the narrowing occurs only at photon energy region higher than the resonance. The reason is not clear and will be correlated with the mechanism of the intensity switching.

The width of the LUMO+2 peak becomes broader with increasing photon energy above the HOMO-LUMO+2 resonance. The width of  $1\omega$  peak should be independent of the photon energy when a fixed intermediate state is assumed. Sakaue predicted that hole scattering causes a broadening of  $1\omega$  peak at photon energy region higher than resonance.<sup>11</sup> According to the theory, the hole partially exists in the bulk band. As the photon energy increases, the hole is formed at deeper energy to fulfill the energy conservation. As a result of the increased phase space to fill the hole, the lifetime of the intermediate state becomes shorter and the  $1\omega$  peak becomes broader. The mechanism seems to be helpful to consistently understand the broadening of the LUMO+2 peak and also the appearance of the peak at the photon energy region high above the resonance. The discussion also leads to a conclusion that the LUMO+2 level observed in 2PPE spectroscopy is not a molecular exciton in which the hole and electron are localized within a molecule. On the other hand, the theory cannot interpret the intensity switching.

### C. L0 and L1 features

The intensity ratio of the split components, L0 and L1, changes with the photon energy increase as can be seen in Fig. 2. The change can be understood by considering resonant excitations from occupied levels deeper than HOMO-1. Fig. 8 shows energy levels for a free PbPc molecule obtained by the DFT calculation and the 2PPE spectra measured at selected photon energies. The energy scale for the calculated levels was adjusted to reproduce the initial energies of the HOMO and HOMO-1 peaks. The occupied levels deeper than HOMO-1 are grouped as (A) to (C). The lengths of vertical arrows are proportional to the photon energies used in the upper 2PPE spectra. The resonance from HOMO-1 to the graphite  $\pi^*$ -band, discussed in Sec. IV A, is shown by an open gray arrow. At low  $h\nu$  of 4.04 eV, the L0 and L1 levels are not resonant with any occupied levels. The resultant 2PPE peaks are weak. The photon energy of 4.18 eV is sufficient to resonantly excite the L0 and L1 levels from the occupied levels of the group (A) and the intensities of the 2PPE peaks become higher. The L1 component is higher than the L0 component by favorable resonance from the high-lying level of the group. At slightly higher photon energy of 4.38 eV, other occupied levels labeled (B) participate in the initial states to excite the L0 level. The intensity ratio of the L0 and L1 components is reversed by the contribution.

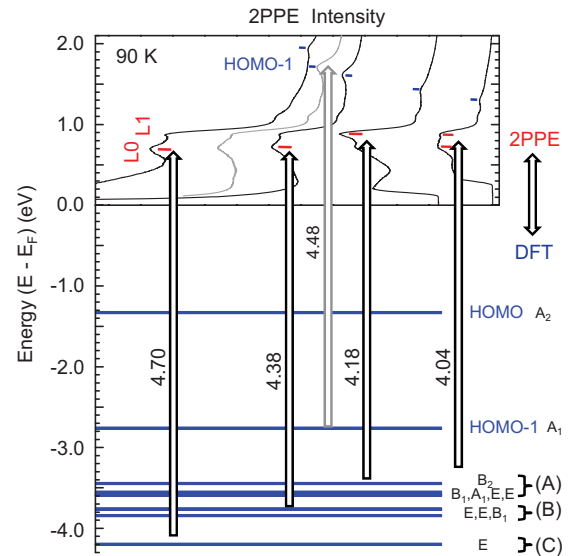


FIG. 8. (Color online) Photon energy dependence of 2PPE spectra at the L0 and L1 region (top) and the energy levels of a free PbPc molecule obtained by the DFT calculation (bottom). The lengths of the vertical arrows are proportional to the photon energies of the 2PPE spectra. The intensity variations in the L0 and L1 peaks are interpreted by the resonant excitations from deeper occupied levels shown by groups of (A) to (C).

At  $h\nu=4.70$  eV, the group (C) occupied levels participate in the initial states to populate the L0 and L1 levels resulting in the increased intensity and the change of the spectral features. Thus the L0 and L1 levels are considered to be populated by resonant excitations from the occupied levels. The resonant 2PPE spectroscopy is effective to resolve the congested occupied levels which cannot be resolved in 1PPE.

### V. CONCLUSION

Photon energy variable 2PPE spectroscopy is effective to reveal detailed resonant excitation processes in the molecule-adsorbed surface. It is interesting that the intensity variations of  $1\omega$  and  $2\omega$  peaks are different for the transitions: only the HOMO-1 peak appears for the resonance between the HOMO-1 level and the  $\pi^*$  band. Intensity switching and the broadening of the  $1\omega$  peak are observed for the HOMO-LUMO+2 resonance. The HOMO-IPS resonance is rather similar to the known trend. The intensity switching and the broadening of the  $1\omega$  peak provide a clear evidence of the unresolved signal generation mechanisms for 2PPE process. The phenomena should generally occur for surfaces on which energy levels of narrow width interact with continuous energy band of the substrate. The present results provide the direction to refine the understanding of 2PPE processes. Deeper understanding of the intensity and width variations is also crucial for advancing 2PPE spectroscopy to a versatile method to probe unoccupied energy levels. Detailed understanding of the nature of the unoccupied levels observed in 2PPE experiment is indispensable when the 2PPE results are compared with other experimental results such as inverse photoemission, optical spectroscopy and so

on. It is also demonstrated that resonant 2PPE spectroscopy is effective to probe not only unoccupied levels but also occupied levels which are buried in complicated 1PPE features.

#### ACKNOWLEDGMENTS

This work was partly supported by Grant-in-Aid for Sci-

entific Research on Priority Areas from MEXT (Grant No. 17069012). The authors are grateful to N. Ueno of Chiba University for supply of PbPc sample, preparation methods of uniform films, and detailed information on his recent works. Global COE Program at Osaka University is acknowledged for partial support to M.S.

- 
- \*Corresponding author. FAX: +81-6-6850-5779; munakata@ch.wani.osaka-u.ac.jp
- <sup>1</sup>H. Ishii, K. Sugiyama, E. Ito, and K. Seki, *Adv. Mater.* **11**, 605 (1999).
  - <sup>2</sup>N. Ueno and S. Kera, *Prog. Surf. Sci.* **83**, 490 (2008).
  - <sup>3</sup>M. Muntwiler, Q. Yang, W. A. Tisdale, and X.-Y. Zhu, *Phys. Rev. Lett.* **101**, 196403 (2008).
  - <sup>4</sup>A. G. Borisov, V. Sametoglu, A. Winkelmann, A. Kubo, N. Pontius, J. Zhao, V. M. Silkin, J. P. Gauyacq, E. V. Chulkov, P. M. Echenique, and H. Petek, *Phys. Rev. Lett.* **101**, 266801 (2008).
  - <sup>5</sup>P. M. Echenique, R. Berndt, E. V. Chulkov, Th. Fauster, A. Goldmann, and U. Höfer, *Surf. Sci. Rep.* **52**, 219 (2004).
  - <sup>6</sup>J. Stähler, M. Meyer, D. O. Kusmirek, U. Bovensiepen, and M. Wolf, *J. Am. Chem. Soc.* **130**, 8797 (2008).
  - <sup>7</sup>K. Boger, M. Roth, M. Weinelt, Th. Fauster, and P.-G. Reinhard, *Phys. Rev. B* **65**, 075104 (2002).
  - <sup>8</sup>H. Ueba, *Surf. Sci.* **334**, L719 (1995).
  - <sup>9</sup>H. Ueba and T. Mii, *Appl. Surf. Sci.* **169-170**, 63 (2001).
  - <sup>10</sup>H. Ueba and B. Gumhalter, *Prog. Surf. Sci.* **82**, 193 (2007).
  - <sup>11</sup>M. Sakaue, T. Munakata, H. Kasai, and A. Okiji, *Phys. Rev. B* **68**, 205421 (2003).
  - <sup>12</sup>W. Wallauer and Th. Fauster, *Surf. Sci.* **374**, 44 (1997).
  - <sup>13</sup>M. Kutschera, M. Weinelt, M. Rohlfing, and T. Fauster, *Appl. Phys. A: Mater. Sci. Process.* **88**, 519 (2007).
  - <sup>14</sup>K. Shudo, S. Takeda, and T. Munakata, *Phys. Rev. B* **65**, 075302 (2002).
  - <sup>15</sup>K. Shudo and T. Munakata, *Phys. Rev. B* **63**, 125324 (2001).
  - <sup>16</sup>I. Yamamoto, M. Mikamori, R. Yamamoto, T. Yamada, K. Miyakubo, N. Ueno, and T. Munakata, *Phys. Rev. B* **77**, 115404 (2008).
  - <sup>17</sup>M. Shibuta, K. Yamamoto, K. Miyakubo, T. Yamada, and T. Munakata, *Phys. Rev. B* **80**, 113310 (2009).
  - <sup>18</sup>T. Munakata, M. Shibuta, M. Mikamori, T. Yamada, K. Miyakubo, T. Sugiyama, and Y. Sonoda, *Proc. SPIE* **6325**, 63250M (2006).
  - <sup>19</sup>I. Yamamoto, N. Matsuura, M. Mikamori, R. Yamamoto, T. Yamada, K. Miyakubo, N. Ueno, and T. Munakata, *Surf. Sci.* **602**, 2232 (2008).
  - <sup>20</sup>S. Kera, H. Fukagawa, T. Kataoka, S. Hosoumi, H. Yamane, and N. Ueno, *Phys. Rev. B* **75**, 121305(R) (2007).
  - <sup>21</sup>Y. Wang, J. Kröger, R. Berndt, and W. Hofer, *Angew. Chem. Int. Ed.* **48**, 1261 (2009).
  - <sup>22</sup>H. Karacuban, M. Lange, J. Schaffert, O. Weingart, Th. Wagner, and R. Möller, *Surf. Sci.* **603**, L39 (2009).
  - <sup>23</sup>J. Lehmann, M. Merschorf, A. Thon, S. Voll, and W. Pfeiffer, *Phys. Rev. B* **60**, 17037 (1999).
  - <sup>24</sup>B. Reihl, J. K. Gimzewski, J. M. Nicholls, and E. Tosatti, *Phys. Rev. B* **33**, 5770 (1986).
  - <sup>25</sup>I. Schäfer, M. Schlüter, and M. Skibowski, *Phys. Rev. B* **35**, 7663 (1987).
  - <sup>26</sup>R. Claessen, H. Carstensen, and M. Skibowski, *Phys. Rev. B* **38**, 12582 (1988).
  - <sup>27</sup>F. Maeda, T. Takahashi, H. Ohsawa, S. Suzuki, and H. Suematsu, *Phys. Rev. B* **37**, 4482 (1988).
  - <sup>28</sup>G. Moos, C. Gahl, R. Fasel, M. Wolf, and T. Hertel, *Phys. Rev. Lett.* **87**, 267402 (2001).
  - <sup>29</sup>K. Sugawara, T. Sato, S. Souma, T. Takahashi, and H. Suematsu, *J. Phys. Chem. Solids* **69**, 2996 (2008).
  - <sup>30</sup>V. M. Silkin, J. Zhao, F. Guinea, E. V. Chulkov, P. M. Echenique, and H. Petek, *Phys. Rev. B* **80**, 121408(R) (2009).
  - <sup>31</sup>K. Ishioka, M. Hase, M. Kitajima, L. Wirtz, A. Rubio, and H. Petek, *Phys. Rev. B* **77**, 121402(R) (2008).
  - <sup>32</sup>H. Petek and S. Ogawa, *Prog. Surf. Sci.* **56**, 239 (1997).
  - <sup>33</sup>E. Knoesel, A. Hotzel, and M. Wolf, *Phys. Rev. B* **57**, 12812 (1998).
  - <sup>34</sup>H. Petek, H. Nagano, M. J. Weida, and S. Ogawa, *Chem. Phys.* **251**, 71 (2000).
  - <sup>35</sup>A. Winkelmann, W.-C. Lin, C.-T. Chiang, F. Bisio, H. Petek, and J. Kirschner, *Phys. Rev. B* **80**, 155128 (2009).
  - <sup>36</sup>R. L. Lingle, Jr., N.-H. Ge, R. E. Jordan, J. D. McNeill, and C. B. Harris, *Chem. Phys.* **205**, 191 (1996).
  - <sup>37</sup>J. D. McNeill, R. L. Lingle, Jr., R. E. Jordan, D. F. Padowitz, and C. B. Harris, *J. Chem. Phys.* **105**, 3883 (1996).
  - <sup>38</sup>W. Berthold, F. Rebentrost, P. Feulner, and U. Höfer, *Appl. Phys. A: Mater. Sci. Process.* **78**, 131 (2004).
  - <sup>39</sup>A. Hotzel, G. Moos, K. Ishioka, M. Wolf, and G. Ertl, *Appl. Phys. B: Lasers Opt.* **68**, 615 (1999).
  - <sup>40</sup>M. Kutschera, T. Groth, C. Kentsch, I. L. Shumay, M. Weinelt, and Th. Fauster, *J. Phys.: Condens. Matter* **21**, 134006 (2009).